ISSN 1063-7834, Physics of the Solid State, 2006, Vol. 48, No. 4, pp. 700–704. © Pleiades Publishing, Inc., 2006.
Original Russian Text © G.S. Patrin, V.V. Beletskiĭ, D.A. Velikanov, O.A. Bayukov, V.V. Vershinin, O.V. Zakieva, T.N. Isaeva, 2006, published in Fizika Tverdogo Tela, 2006, Vol. 48, No. 4, pp. 658–662.

MAGNETISM
AND FERROELECTRICITY

# Nonstoichiometry and Low-Temperature Magnetic Properties of FeSi Crystals

**G. S. Patrin[a, b], V. V. Beletskiĭ[b], D. A. Velikanov[a], O. A. Bayukov[a], V. V. Vershinin[b], O. V. Zakieva[b], and T. N. Isaeva[a]**

[a] *Kirensky Institute of Physics, Siberian Division, Russian Academy of Sciences, Akademgorodok, Krasnoyarsk, 660036 Russia*
*e-mail: patrin@iph.krasn.ru*
[b] *Krasnoyarsk State University, Krasnoyarsk, 660041 Russia*

Received May 25, 2005

**Abstract**—The results of experimental and theoretical studies of the low-temperature properties of FeSi crystals are presented. The specific features of the magnetic susceptibility are shown to be related to the superparamagnetic behavior of impurity clusters. The thermomagnetic hysteresis phenomena observed are explained using the model of exchange-coupled clusters.

PACS numbers: 75.50.Bb, 75.60.Nt

**DOI:** 10.1134/S1063783406040135

## 1. INTRODUCTION

For a long time, the FeSi crystal has attracted the attention of researchers due to its unique physical properties. This crystal has been found to exhibit unusual behavior of the magnetic susceptibility, thermal, and electrical parameters. For example, as the temperature increases, the electrical resistivity ρ first decreases monotonically by approximately four orders of magnitude, reaches a minimum near $T \approx 300$ K (in this case, $\rho(T)$ cannot be described by a simple thermal-activation dependence), and then slowly increases. Because of this, the FeSi crystal is assigned either to the Kondo compounds [1] or to materials in which a semiconductor–metal transition is realized [2]. In terms of its magnetic properties, this material does not fit the traditional scheme of magnetic behavior. As the temperature increases to $T \approx 90$ K, the magnetic susceptibility decreases ($\chi \sim 10^{-4}$–$10^{-6}$) and then increases significantly and reaches a maximum at $T \approx 500$ K [3]. Mössbauer spectroscopy studies [4] and neutron diffraction analysis [5] have not revealed any magnetic order in this compound. At $T > 550$ K, the temperature dependence of the magnetic susceptibility obeys the Curie–Weiss law. However, more extensive experiments using polarized neutrons [6] have revealed the presence of magnetic scattering, which was interpreted as being due to the existence of microregions with ferromagnetic correlations of spin fluctuations.

The iron ions in this crystal are believed to be in the tetravalent state ($Fe^{4+}$) and have, in the $d^4$ configuration, the ground state $e_{2g}^4$ ($S = 0$). The energy gap between the ground state and the first excited state is $\Delta \sim 600$ K. Therefore, the magnetic moment must be entirely absent at low temperatures and can occur only with increasing temperature, when the $e_{2g}^3 t_{2g}^1$ state ($S = 1$) is filled. In the high-temperature range, the magnetic properties can be adequately described in terms of filling of this level [7]. However, the situation is unclear in the low-temperature range. On the one hand, there is a point of view that the low-temperature specific features can be explained in terms of the presence of impurity-iron ions that occur due to nonstoichiometry of the crystal [3, 8, 9]. On the other hand, the authors of [10–12] interpret the results of complex investigations of the magnetic, thermoelectric, and galvanomagnetic properties of the FeSi crystal in the framework of the Hubbard model with strong electron correlations. The low-temperature specific features of the physical properties are associated in [10–12] with the formation of spin polarons. However, up to now, a universally accepted approach to the description of the complete set of physical properties has been lacking. For this reason, we studied the low-temperature magnetic properties of FeSi samples prepared under various technological conditions.

## 2. SAMPLE PREPARATION AND EXPERIMENTAL TECHNIQUE

We synthesized both polycrystalline samples and single crystals. As is known [13], in the iron–silicon system, the ε-FeSi phase with a zinc-blende structure exists in a narrow region near the equiatomic composition. The polycrystalline samples were produced by melt cooling at a rate of 3 K/h. Preliminarily, a mixture

of iron and silicon was ground thoroughly and then heated to melting and held at this temperature for 5 h. After cooling, the material obtained was again ground and the overall procedure was repeated. Three to four cycles were performed. The single-crystal samples were grown using the standard gas-transport reaction method. The crystallite sizes in samples $O1$ and $O2$ were $\leq 10^{-2}$ mm, and the cross-sectional size of a single crystal (in the form of a tetrahedron) was 1.5 mm. The x-ray diffraction patterns were obtained for several samples taken from different regions of a crucible. The x-ray diffraction data agreed for all of the compositions synthesized.

Magnetic measurements were carried out using a SQUID magnetometer in the temperature range $T$ = 4.2–300 K in magnetic fields $H \leq 0.8$ kOe and also using a high-temperature vibrating-coil magnetometer operating at temperatures of up to $T \approx 950$ K.

## 3. EXPERIMENTAL RESULTS

Below, we present the experimental data obtained on FeSi (sample $O1$) and $Fe_{1.005}Si_{0.995}$ (sample $O2$) polycrystals and a single crystal. Figure 1 shows the x-ray diffraction patterns for samples $O1$ and $O2$; these data are in agreement with the literature data. The spectra of these samples are seen to be closely similar even in terms of their details; namely, the peak positions and intensities are coincident, with the exception of the peak intensities at large scattering angles. Since these peaks occur due to x-ray scattering from the planes with small interplanar spacings, the observed difference indicates that the nearest surrounding of iron ions varies with the ratio between the chemical elements in a sample. The x-ray diffraction pattern for the single-crystal sample is virtually the same as that for sample $O1$.

Figure 2 shows the temperature dependences of the magnetic susceptibility of samples $O1$ and $O2$ and the FeSi single crystal (curves *1–3*, respectively). It is worth noting that, under the same experimental conditions, the magnetic susceptibility of polycrystalline sample $O1$ (which is nominally stoichiometric) is lower than that of sample $O2$. The difference between the temperature dependences of the susceptibility for different samples decreases as the magnetic field increases ($H \longrightarrow 10$ kOe). On the whole, the magnetic susceptibility versus temperature curve for sample $O1$ has the form shown in the inset to Fig. 2. This dependence is typical of the FeSi compound.

It was established that external influences manifest themselves to the greatest extent for the a priori defect sample $O2$. For this reason, we studied this sample in more detail. The emphasis was on studying the low-field specific features in the behavior of the magnetization. The magnetization curves were measured as functions of the thermomagnetic prehistory. Figure 3 shows the variation in the magnetization measured in both

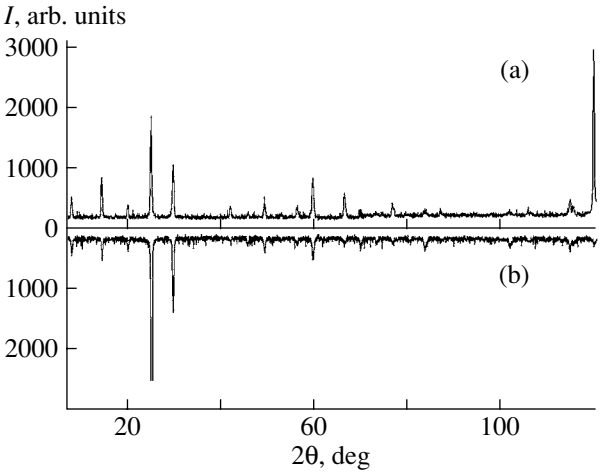


**Fig. 1.** X-ray diffraction patterns of FeSi crystals: (a) a sample with an equiatomic iron and silicon content ($O1$) and (b) a sample with an excess iron content ($O2$).

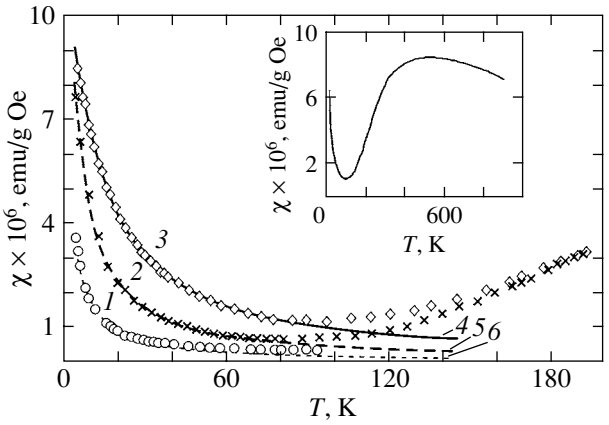


**Fig. 2.** Temperature dependences of the magnetic susceptibility for (*1*, *2*) FeSi polycrystalline samples $O1$ and $O2$, respectively, and (*3*) an FeSi single crystal. Points *1–3* show experimental data, and lines *6*, *5*, and *4* are the respective theoretical fittings with a Langevin function. The measurement field is $H$ = 600 Oe. The inset shows the temperature dependence of the magnetic susceptibility in the entire temperature range possible for sample $O1$.

increasing and decreasing fields for sample $O2$ cooled in a zero magnetic field. It is seen that, in the magnetic-field range studied, saturation is not reached, which agrees with other experimental data obtained in high magnetic fields [11]. In magnetic fields $H \leq 150$ Oe at $T$ = 4.2 K, pronounced hysteresis is observed in the magnetization curve for sample $O2$, whereas for sample $O1$ and the single crystal the hysteresis is less by approximately one order of magnitude. In the initial portion of the curve, the behavior of the magnetization is obviously different from that for a paramagnet and is characteristic of a system with interactions.

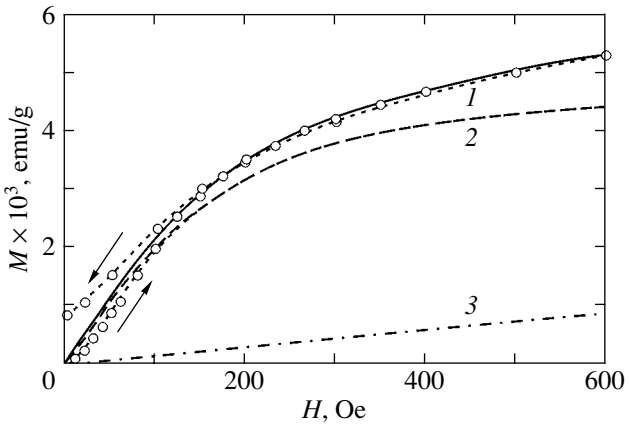


**Fig. 3.** Field dependences of the magnetization for sample *O*2. The arrows indicate the sweep direction of the magnetic field. Points are experimental data, curves *1* are theoretical fittings (the solid curve is a Langevin function), and curves *2* and *3* correspond to the data set for sample *O*2 from the table. $T = 4.2$ K.

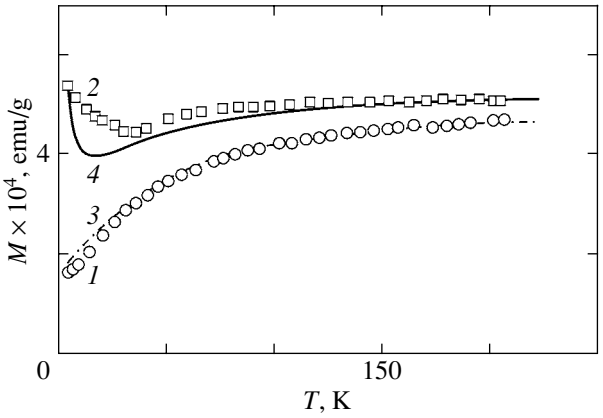


**Fig. 4.** Temperature dependences of the magnetization for sample *O*2. Points are experimental data, and lines correspond to calculations performed for (*1*, *3*) the ZFC regime and (*2*, *4*) the FC regime. The measurement field is $H$ = 10 Oe.

Figure 4 shows the temperature dependences of the low-field magnetization for sample *O*2 obtained during cooling in a zero magnetic field (the ZFC regime) and in a measurement field $H = 10$ Oe (the FC regime). As follows from Fig. 4, the most substantial distinctions between the $M(T)$ curves are observed up to a temperature $T \approx 100$ K, which corresponds to the minimum in the temperature dependence of the magnetization. At higher temperatures, the curves approach each other and their behaviors become similar. The higher the measurement field, the less the observed distinctions between the $M(T)$ curves and the lower the temperature at which the distinction between the magnetization curves obtained under different cooling conditions is observed.

To reveal magnetically ordered regions, we also performed Mössbauer spectra measurements of the natural iron content in powder samples 5 mg/cm$^2$ thick. The spectra are found to be paramagnetic doublets. We obtained the following parameters of the hyperfine structure: the isomer chemical shift with respect to α-Fe is $\delta = 0.27 \pm 0.01$ mm/s, the hyperfine field at the iron nucleus site is $H_{fs} = 0$, the quadrupole splitting is $\varepsilon = 0.5 \pm 0.02$ mm/s, and the linewidth at half-maximum is $W = 0.37 \pm 0.02$ mm/s. From the chemical shift, we estimated the silicon content in the samples to be ≈50 at %. All the above parameter values correspond (within the accuracy of the experiment) to the literature data.

Magnetic moments of iron clusters $m$, the number of atoms in a cluster $n$, and the cluster content in a sample $N$

| Sample | $m$, $10^{-18}$ G | $n$ | $N$, $10^{15}$ cm$^{-3}$ |
|---|---|---|---|
| *O*1 | $m_1 = 2.7$ | $n_1 = 97$ | $N_1 = 2.67$ |
| *O*2 | $m_{21} = 7.5$ | $n_{21} = 270$ | $N_{21} = 0.68$ |
| | $m_{22} = 0.612$ | $n_{22} = 22$ | $N_{22} = 7.07$ |
| Single crystal | $m_3 = 2.2$ | $n_3 = 79$ | $N_3 = 1.52$ |

## 4. DISCUSSION OF THE RESULTS

The experimental results obtained can be interpreted in the framework of the impurity center model. Indeed, an analysis of the literature data shows that the values of both the low-temperature magnetic susceptibility and low-field thermomagnetic hysteresis vary noticeably from sample to sample. In this case, the problem of primary importance is to determine the magnetic moments and the amounts of magnetic impurities (clusters). We fitted the experimental curves in Fig. 2 using the Langevin functions

$$M(H, T) = mN\left\{\coth\left(\frac{mH}{k_B T}\right) - \frac{k_B T}{mH}\right\}, \qquad (1)$$

where $k_B$ is the Boltzmann constant and $H$ is the measurement field (in our case, $H = 600$ Oe). The magnetic moments $m$ of impurity clusters and the content of clusters $N$ are considered to be adjustable parameters. We found that experimental curves *1* and *3* in Fig. 2 fit function (1) well (curves *6* and *4* in Fig. 2, respectively) and that curve *2* fits a superposition of two functions (1) (curve *5* in Fig. 2). The table lists the values of the magnetic moments $m$, the number of atoms in a cluster $n$, and the content of impurity clusters $N$ in the samples studied.

When determining the number of atoms in a cluster $n$, we used the results from [14], where the magnetic properties of iron clusters were calculated as a function of the number of particles in a cluster. From that calculation, it follows that, as the cluster size increases, the magnetic moment per atom increases and becomes equal to about $3\mu_B$ (as in bulk iron) for clusters containing 15 or more atoms. It is known [2] that the FeSi crys-

tal, as well as pure Si, has a zinc-blende structure with a lattice parameter $a = 0.484$ nm. The unit cell contains four formula units. Therefore, the total number of iron atoms per 1 cm$^3$ is $3.5 \times 10^{22}$ and only ~$3 \times 10^{17}$ of them (for sample *O*2) are in clusters. In this case, the average interparticle spacing is $r_{ij} \sim 50$ nm if the average cross-sectional size of the particles is $d \leq 1$ nm. For compounds with this structure, in particular, for silicon [15], the formation of structural defects (precipitates) up to 50 nm in size is typical.

Thus, we can conclude that, in fields $H > 100$ Oe, the system behaves like an ensemble of superparamagnetic particles. However, the behavior in low magnetic fields invites special discussion. In principle, the dipole–dipole interaction between superparamagnetic particles [16] can give rise to thermomagnetic hysteresis phenomena. However, in our case, estimating the contribution from the dipole–dipole interaction to the molecular field ($H_{dd} \sim m/r_{ij}^3$) gives a maximum value $H_{\rm dd} \approx 0.5$ Oe, which cannot explain the experimental results.

Experimental dependences *1* and *2* in Fig. 4 are the most demonstrative. These dependences can be fitted by the following empirical curves:

(a) curve *3*

$$M(H, T)_{\rm ZFC} = M_{22}(T, h)N_{\rm ZFC} + M_{\rm res}, \qquad (2)$$

where $h = H - 1900$ Oe is the effective field acting on a cluster $m_{22}$, $H = 10$ Oe is the measurement field, $M_{22}(T, h)$ is the Langevin function for clusters of size $n_{22}$, and $M_{\rm res} \approx M_2(T = 80\ {\rm K}, H = 600\ {\rm Oe})$ is the remanent magnetization;

(b) curve *4*

$$M(T, H)_{\rm FC} = M_2(T, H) + M_{22}(T, h)N_{\rm FC} + M_{\rm res}, \quad (3)$$

where $N_{\rm ZFC} = 8 \times 10^{-2}$ and $N_{\rm FC} = 6 \times 10^{-2}$ are the fractions of clusters involved in the interaction under the conditions corresponding to Fig. 4.

These dependences can be explained if it is assumed that the impurity clusters are segregated [15] and some large clusters of size $n_{21}$ are surrounded by smaller clusters of size $n_{22}$ that are in immediate contact with the large clusters. Let $m_{1l}$ and $m_{2i}$ be the cluster magnetic moments that do not interact and let $m_{1k}$ and $m_{2j}$ be the cluster magnetic moments that are coupled via exchange interaction. Here, indices 1 and 2 refer to the clusters of sizes $n_{21}$ and $n_{22}$, respectively. In this case, the energy of the overall system can be written in the form

$$E = E_{\rm SP} + E_{\rm int},$$

where

$$E_{\rm SP} = -\left(\sum_l \mathbf{m}_{1l} + \sum_i \mathbf{m}_{2i}\right)\mathbf{H} \qquad (4)$$

describes the superparamagnetic part of the system (the indices $l$ and $i$ label the noninteracting clusters) and

$$E_{\rm int} = -\left(\sum_k \mathbf{m}_{1k} + \sum_j \mathbf{m}_{2j}\right)\mathbf{H} + \sum_{k,j} \lambda \mathbf{m}_{1k}\mathbf{m}_{2j} \qquad (5)$$

describes the interacting part of the system (the indices $k$, $j$). Here, the parenthetical expression is the Zeeman contribution from the clusters with sizes $n_{21}$ and $n_{22}$; the last sum describes the exchange interaction between these clusters; and $\lambda$ is the exchange interaction constant, which is taken to be the same for all pairs for simplicity. It follows from formula (2) that the molecular field $h_{\rm MF}$ that acts on the $j$th cluster belonging to the $n_{22}$ set corresponds to antiferromagnetic exchange. The value of this field can be determined from Eq. (5) as $(\mathbf{h}_{\rm MF})_{2j} = \mathbf{H} - \lambda \mathbf{m}_{1k}$ ($\lambda > 0$), where $\lambda m_{1k} = 1900$ Oe.

On cooling in a zero magnetic field (ZFC regime), each cluster from the $n_{21}$ set with index $k$ is oriented randomly. Therefore, the magnetization of this subsystem and, as a result, the average magnetization of the clusters $n_{22}$ with index $j$ that are exchange-coupled with the above clusters are equal to zero. After a weak magnetic field is applied, in the subsystem $m_{1k} \neq 0$ and, owing to the inequality $|\lambda m_{1k}| \gg H$, clusters $m_{2j}$ are oriented in the direction opposite to the external magnetic field. Further, as the temperature increases, the contribution of this subsystem to the total magnetization decreases on the background of the remanent magnetization; as a result, we obtain curves *1* and *3* in Fig. 4. In the case of cooling in a magnetic field (FC regime), the total magnetization of the superparamagnetic subsystem is noticeably higher than the remanent magnetization and curves *2* and *4* in Fig. 4 are obtained as a result of summation of the magnetizations of the superparamagnetic and exchange-coupled subsystems. The value and behavior of the remanent magnetization cannot be explained using this idealized system. It is likely that we should take into account the iron ions of the host matrix, which interact with the iron clusters at the boundaries. In the initial range of the temperature dependence of the magnetization of the host iron ions, its value is determined by the population of the excited state $\exp(-\Delta/k_BT)/[1 + \exp(-\Delta/k_BT)]$. It is easy to find that, at $T \approx 100$ K, the population is $2.5 \times 10^{-3}$ and the magnetization of the host matrix at this temperature is higher than that of the cluster subsystem. The interaction between the cluster subsystem and the host iron ions can induce metastable states, which will cause remanent phenomena.

## 5. CONCLUSIONS

As a result of the study performed, we have established that the low-temperature magnetic susceptibility of the FeSi crystal is associated with the superparamagnetic state of the clusters formed due to nonstoichiometry. The thermomagnetic remanent phenomena have

been explained under the assumption that exchange coupling exists between part of the magnetic clusters. In more perfect polycrystalline samples and single crystals, the size distribution of clusters has a small spread, as indicated by the good fitting of the experimental data with a Langevin function (although accidental coincidence cannot be ruled out). High nonstoichiometry provides a spreading of the size distribution and makes simple description of the experimental data impossible. In this case, an excess content of the impurity iron leads to the formation of new nuclei of smaller size rather than to cluster growth.

## ACKNOWLEDGMENTS

This work was supported by the Russian Foundation for Basic Research (RFBR–Yenisei program), project no. 05-02-977708-a.

## REFERENCES

1. G. Aeppli and Z. Fisk, Comments Condens. Matter Phys. **16**, 155 (1992).
2. M. Imada, A. Fujimori, and Y. Tokura, Rev. Mod. Phys. **70**, 1039 (1998).
3. V. Jaccarino, G. K. Wertheim, J. H. Wernick, L. R. Walker, and S. Arajs, Phys. Rev. **160**, 476 (1967).
4. G. K. Wertheim, V. Jaccarino, J. H. Wernick, J. A. Seitchik, H. J. Williams, and R. S. Sherwood, Phys. Lett. **18**, 89 (1965).
5. M. Kohgi and Y. Ishikawa, Solid State Commun. **37**, 833 (1981).
6. K. Tajima, Y. Endoh, J. E. Fisher, and G. Shirane, Phys. Rev. B: Condens. Matter **38**, 6954 (1988).
7. T. Moriya, *Spin Fluctuations in Itinerant Electron Magnetism* (Springer, Berlin, 1985; Mir, Moscow, 1988).
8. M. Mihalik, M. Timko, P. Samuely, N. Tomašovičova-Hudákova, P. Szabo, and A. A. Menovsky, J. Magn. Magn. Mater. **157/158**, 637 (1996).
9. B. C. Sales, E. C. Jones, B. C. Chakoumakos, J. A. Fernandes-Baca, H. E. Harmon, J. W. Sharp, and E. H. Volckmann, Phys. Rev. B: Condens. Matter **50**, 8207 (1994).
10. N. E. Sluchanko, V. V. Glushkov, S. V. Demishev, M. V. Kondrin, K. M. Petukhov, N. A. Samarin, V. V. Mochalkov, and A. A. Menovsky, Europhys. Lett. **51**, 557 (2000).
11. N. E. Sluchanko, V. V. Glushkov, S. V. Demishev, M. V. Kondrin, V. Yu. Ivanov, K. M. Petukhov, N. A. Samarin, A. A. Menovsky, and V. V. Moshchalkov, Zh. Éksp. Teor. Fiz. **119** (2), 359 (2001) [JETP **93** (2), 312 (2001)].
12. N. E. Sluchanko, V. V. Glushkov, S. V. Demishev, A. A. Menovsky, L. Weckhusen, and V. V. Mochalkov, Phys. Rev. B: Condens. Matter **65**, 064 404 (2002).
13. G. V. Samsonov, L. A. Dvorina, and B. V. Rud', *Silicides* (Metallurgiya, Moscow, 2003) [in Russian].
14. C. Y. Yang, K. H. Johnson, D. S. Salagub, J. Kaspar, and R. P. Messner, Phys. Rev. B: Condens. Matter **24**, 5673 (1981).
15. Yu. Yu. Loginov, P. D. Brown, and K. Durose, *Formation of Structural Defects in II–VI Semiconductors* (Logos, Moscow, 2003) [in Russian].
16. V. P. Shcherbakov and V. V. Shcherbakova, Izv. Akad. Nauk SSSR, Fiz. Zemli **6**, 69 (1977).

*Translated by Yu. Ryzhkov*